

## DOUBLE-LABEL COUNTING OF HETEROGENEOUS SAMPLES

AGUSTIN GRAU CARLES, LEONOR RODRÍGUEZ BARQUERO  
and AGUSTIN GRAU MALONDA

Instituto de Investigación Básica, Centro de Investigaciones Energéticas, Medioambientales y Tecnológicas (CIEMAT), Avenida Complutense 22, E-28040 Madrid, Spain

**ABSTRACT.** We describe sample preparation of gels with a given sample quenching parameter (SQP(E)). The procedure is applied to mixtures of  $^{45}\text{Ca}$  and  $^{35}\text{S}$  with activity ratios from 25/1 to 1/20 and quench values that make  $^{35}\text{S}$  efficiency range from 63% to 88%. We compare the two-window and unfolding methods. Low-level activity mixtures are standardized by a spectrum unfolding method. We also studied components with counting rates below background and show that the CIEMAT/NIST method yields excellent results with gels.

### INTRODUCTION

Adsorption may cause instability problems when homogeneous samples are assayed in liquid scintillation counting (LSC). Generally, these problems can be resolved by adding an acid or a carrier to the solution. The presence of color can introduce further errors, which we address by confining the radioactive solution in micromicelles inside the scintillator. In this way, we avoid adsorption by the vial walls. Some commercial scintillators, such as Insta-Gel®, facilitate the preparation of heterogeneous solutions by adding adequate amounts of water to the scintillator. The term "heterogeneous solution" is not well defined, and its use may lead to confusion. Some investigators consider a heterogeneous solution to be a mixture of clearly separated phases. Others define the term as a mixture of solids and liquids. We define a heterogeneous solution as a gel in which water is confined in micelles. Unexpectedly, we observed that standardization curves do not depend on the water content of the samples, and they do not differ from homogeneous samples. In other words, standardization curves do not depend on the size of the micromicelles inside the scintillator.

Several researchers applied the Centro de Investigaciones Energéticas, Medioambientales y Tecnológicas/National Institute of Standards and Technology (CIEMAT/NIST) method (Grau Malonda 1982a,b; Grau Malonda & García-Toraño 1982; Coursey *et al.* 1989; Günter & Schötzig 1992; Rodriguez, Los Arcos & Grau 1991) to homogeneous samples. We found that the CIEMAT/NIST method can be applied to homogeneous samples as well as to gels. Although the standardization curves do not depend on the water content, the counting efficiency and sample quenching parameter (SQP(E)) decrease as the volume ratio water/scintillator increases. We used carbon tetrachloride to obtain samples with different water content, but the same SQP(E) values, and unexpectedly, the counting efficiency was the same, *i.e.*, the counting efficiency depends only on SQP(E), and the water/scintillator ratio does not affect the final standardization curve. Despite the fact that water content is unimportant for standardizing a radionuclide by the CIEMAT/NIST method, we studied the simultaneous effects of water and carbon tetrachloride on quenching to obtain rapidly quenched gel samples with given SQP(E). We derive expressions for calculating SQP(E) as a function of the amount of water and carbon tetrachloride incorporated in the vials. We also analyzed  $^3\text{H}$ ,  $^{35}\text{S}$ ,  $^{45}\text{Ca}$  pulse-height spectra with different water proportions, but with the same SQP(E). The results confirm that spectra from homogeneous and heterogeneous samples are identical when they have the same characteristic SQP(E) value. In fact, spectral shapes depend only on SQP(E), which allows us to apply the spectrum unfolding method (Grau Carles & Grau Malonda 1991a,b; Grau Carles, Martín-Casallo & Grau Malonda 1991) to heterogeneous mixtures.

We have obtained excellent results using the spectrum unfolding method, especially when spectral overlap is important. We discuss here the spectrum unfolding method applied to  $^{45}\text{Ca}$  and  $^{35}\text{S}$  heterogeneous mixtures, and we compare some of the results with the double-window method. We also analyze medium- and low-activity samples, and indicate the potential of the spectrum unfolding method.

## METHODS

We used an LKB Rackbeta 1219 Spectral LS spectrometer for the measurements. The system has a  $^{226}\text{Ra}$  source for quench determination by the external standard method. All the measurements were made at a temperature of  $16^\circ\text{C}$ . Low-potassium glass vials were used in all cases. Combined carrier and acid were used to obtain stable radioactive solutions. Because  $^{45}\text{CaCl}_2$  dissolved in water is adsorbed by the walls, we added 1M HCl and 257 mg  $\text{Ca}^{2+} \text{ ml}^{-1}$  to avoid this, and used 0.5M  $\text{H}_2\text{SO}_4$  for  $\text{H}_2^{35}\text{SO}_4$ .

One virtue of using gels is that they are easy to prepare, and require no gravimetric deposition. Volumes of radioactive substance can be dispensed with a pipette. The heterogeneous standards were prepared by pipetting 5 ml of the radioactive solution into vials containing 10 ml of scintillator. The vials were shaken and left at  $16^\circ\text{C}$  for 4 h before measurement. Samples with different quench values and with the same water/scintillator ratio were obtained by adding  $\text{CCl}_4$  to the scintillator before the radioactive solution was incorporated.

Addition of  $\text{CCl}_4$  to the gel does not increase quench. The  $\text{CCl}_4$  must be added while water and scintillator are in separate phases. The phases will separate in the vials after 10 min at  $35^\circ\text{C}$ .  $\text{CCl}_4$  can be added later and the gel reconstituted by shaking and cooling the vials at  $16^\circ\text{C}$ . In this way, we were able to increase quench stepwise on the same sample.

Nine  $^{45}\text{Ca}$  and  $^{35}\text{S}$  standards were prepared to test the CIEMAT/NIST procedure in heterogeneous solutions. Figure 1 shows experimental points and computed calibration curves. The same water/scintillator ratios were used in all samples to obtain the calibration curves, although other ratios are possible. Even when they have different water/scintillator ratios, all quench vs. efficiency points are on the same calibration curve. Care was taken to use the same total volume throughout the experiment. It is common to employ experimental curves that relate the quencher volumes used and the SQP(E). We plotted one of these curves in Figure 2A. When  $\text{CCl}_4$  is used as a quencher, the quench ratios follow the law

$$\frac{Q'}{Q} = 1 + \alpha \left( \frac{v}{V} \right)^{3/4} + \beta \left( \frac{v}{V} \right)^{3/2} \quad (1)$$

where  $Q$  is the SQP(E) value for the unquenched Insta-Gel®, and  $Q'$  is the SQP(E) obtained when a volume,  $v$ , of quencher is added.  $V$  is the volume of Insta-Gel® (10 ml) and alpha and beta are constants. The curve in Figure 2A exhibits linear behavior for small-volume additions of quencher

$$\frac{Q'}{Q} = 1 + \mu \left( \frac{v}{V} \right)^{3/4} . \quad (2)$$

In the same manner, one should obtain an experimental curve for gels relating the SQP(E) value and the water proportion. The main difficulty is that curves have different behaviors, depending on the quantity of  $\text{CCl}_4$  used before the gel is formed. To illustrate this, we prepared 6 sets of 8

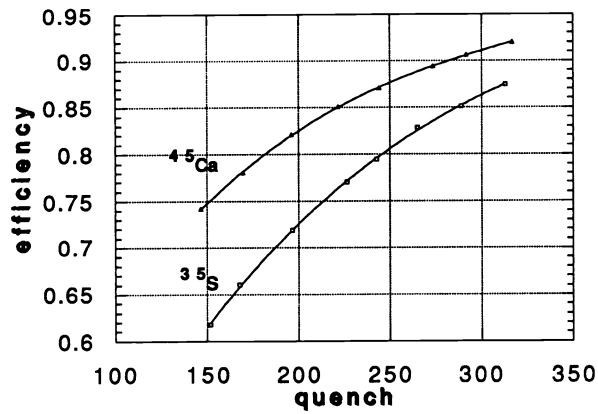


Fig. 1. Calibration curves for  $^{45}\text{Ca}$  and  $^{35}\text{S}$ . The quench parameter is the SQP(E).

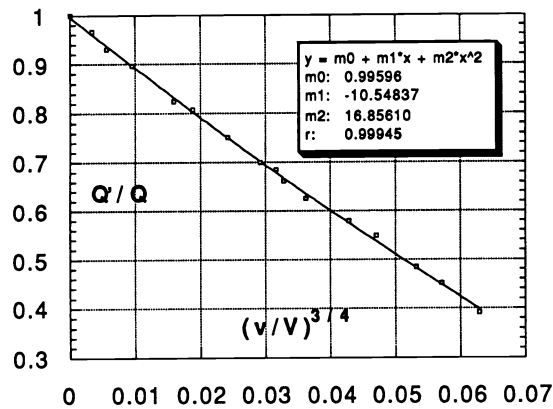


Fig. 2A. Fitted curve of  $(v/V)^{3/4}$  vs.  $Q'/Q$ .  $V$  is the total volume of Insta-Gel® (10 ml),  $v$  the added  $\text{CCl}_4$  volume.  $Q$  is SQP(E) of unquenched Insta-Gel® and  $Q'$  SQP(E) after quencher was added.

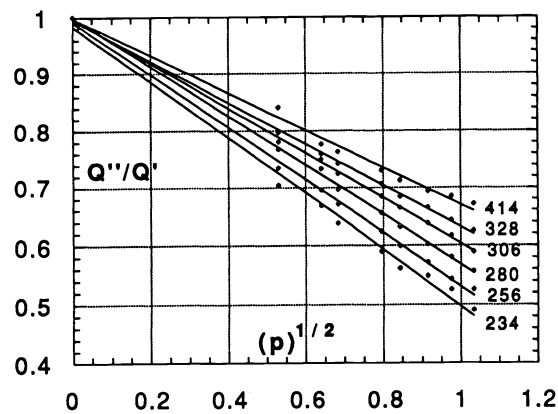


Fig. 2B. Fitted lines of  $(p)^{1/2}$  vs.  $Q''/Q'$ .  $p$  is the water/Insta-Gel® volume ratio,  $Q'$  SQP(E) of Insta-Gel® and  $Q''$  SQP(E) when gel was formed. Depending on added  $\text{CCl}_4$  volume to Insta-Gel®, the slope of the line is different. SQP(E) of Insta-Gel® before water was added are on the right.

samples, depositing 10 ml of Insta-Gel® with the SQP(E) varying from  $Q = 414$ , for the first set of unquenched samples, to  $Q' = 234$ , for the last set of quenched samples, to which we added 0.17 ml of  $\text{CCl}_4$ . We varied the water/Insta-Gel® ratio for each set of samples to obtain the results shown in Figure 2B, where each line represents a different initial quantity of quencher. Although all curves have a different slope, they follow the same law

$$\frac{Q''}{Q'} = 1 + m'(p)^{1/2} \quad (3)$$

where  $p$  is the water/scintillator ratio,  $Q'$ ,  $Q''$  are the SQP(E) for the quenched scintillator and the gel, respectively, and  $m'$  is the observed slope for each line in Figure 2B. All lines plotted in Figure 2B can be related to the line of slope,  $m$ , obtained from the first set of unquenched samples by the empirical expression

$$\frac{Q'}{Q} = 1 + \gamma (m - m')^{1/2} \quad (4)$$

Practical tables can be constructed by using Equations (1), (3) and (4) and the gel-quench value computed from the quencher, scintillator and water volumes. Conversely, a standard with a given quench value can be prepared easily by adding given amounts of water, scintillator and quencher. These tables are of interest in the rapid preparation of gels with a certain SQP(E) and, consequently, in the application of the spectrum unfolding method to radionuclide mixtures. The spectrum unfolding method has already been applied successfully to homogeneous samples (Grau Carles & Grau Malonda 1991a,b; Grau Carles, Martín-Casallo & Grau Malonda 1991). Because pulse-height spectra with the same SQP(E) from homogeneous or heterogeneous samples do not differ, the spectrum unfolding method can be applied to heterogeneous mixtures as well. Due to the presence of water, SQP(E) in homogeneous samples are greater than in heterogeneous samples, resulting in a greater spectral overlap for gels, which often makes the double-window method inapplicable. Table 1 compares discrepancies of experimental and computed activities obtained by both methods.

TABLE 1. Discrepancy between Experimental and Computed Activities of  $^{45}\text{Ca}$  and  $^{35}\text{S}$  By the Unfolding Method (UM) and the Double-Window Method (DWM)

Sample no.	Activity ratio	SQP(E)	Discrepancy (%) (UM)		Discrepancy(%) (DWM)	
			$^{45}\text{Ca}$	$^{35}\text{S}$	$^{45}\text{Ca}$	$^{35}\text{S}$
	$^{45}\text{Ca}/^{35}\text{S}$					
1	10.3/1	171.3	0.3	-6.2	-5.5	17.0
2	4.5/1	170.1	1.9	-12.8	7.5	-40.0
3	1.7/1	171.2	-0.1	-3.9	-7.0	23.0
4	1/1.3	168.9	3.3	4.7	7.4	-8.1
5	1/3.5	169.9	1.1	-2.8	13.0	-6.6
6	1/7.9	169.7	-9.2	-2.9	17.0	-6.7

We applied a spectral interpolation method to determine the  $^{45}\text{Ca}$  and  $^{35}\text{S}$  spectra for the SQP(E) of the mixture. These techniques were described previously (Grau Carles & Grau Malonda 1991a,b; Grau Carles, Martín-Casallo & Grau Malonda 1991). Eight  $^{45}\text{Ca}$  standards (SQP(E) = 316.9, 291.6, 273.5, 243.9, 221.7, 196.0, 169.7, 146.6) and 8  $^{35}\text{S}$  standards (SQP(E) = 313.1, 288.9, 265.1, 242.7, 226.6, 196.6, 167.6, 151.7) were used to carry out the spectral interpolation. Figures 3A and 3B

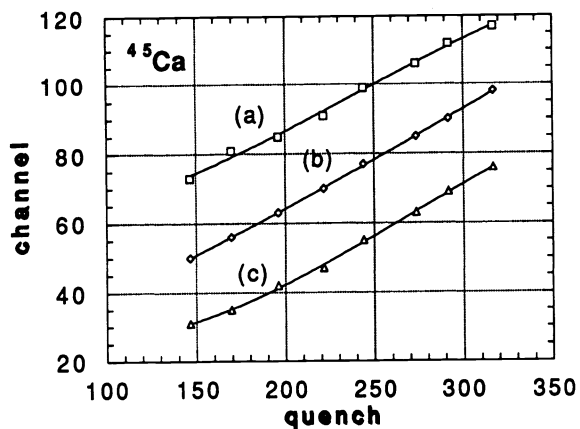


Fig. 3A. Fitted curves of <sup>45</sup>Ca local parameter vs. quench: (a) endpoints of the spectra, (b) inflection points, (c) position of the spectral maxima.

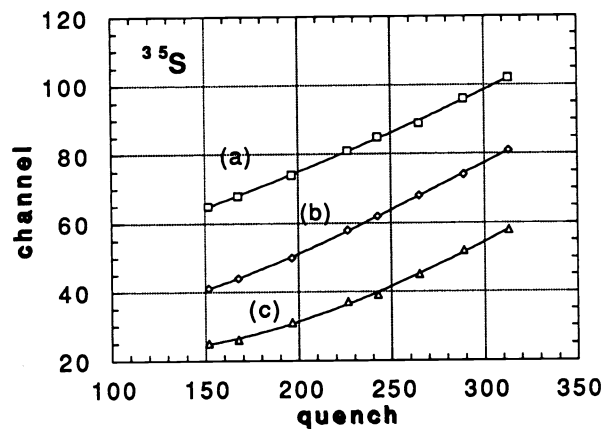


Fig. 3B. Fitted curves of <sup>35</sup>S local parameter vs. quench: (a) endpoints of the spectra; (b) inflection points, (c) position of the spectral maxima.

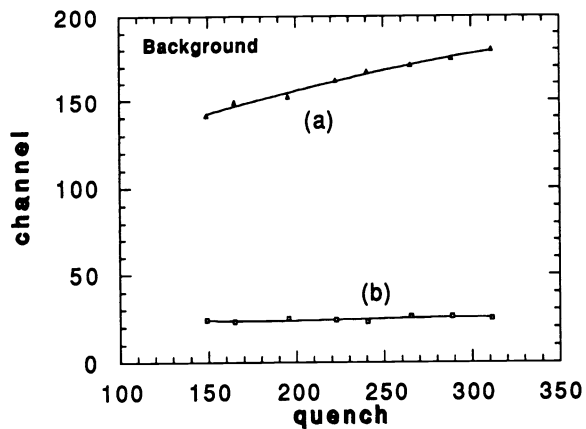


Fig. 3C. Fitted curves of background local parameter vs. quench: (a) endpoints of the spectra (end of cosmic peak); (b) position of the spectral maxima (Cerenkov peak of <sup>40</sup>K).

show the required curves for this procedure, which give the position of the maximum, inflection and endpoint of the spectra as a function of SQP(E).

The advantages of the present spectrum unfolding method are seen when applied to low-activity samples. Low-activity dual samples can be deconvoluted by the spectrum unfolding method by considering the background as a new spectral source component. In such a way, the problem is reduced to a three-spectral component situation. Background components can be obtained by spectral interpolation in background standards with different SQP(E). Analogous curves, as in Figures 3A and 3B for  $^{45}\text{Ca}$  and  $^{35}\text{S}$ , can be plotted from background spectra. Background maxima are determined by the Cerenkov peak of  $^{40}\text{K}$  (present in glass vials); the endpoints of spectra are obtained by the endpoint of the cosmic radiation peak, near 9 MeV. The curves showing the positions of maxima and endpoints of the background spectra vs. SQP(E) values are plotted in Figure 3C.

## RESULTS AND DISCUSSION

Table 2 shows the results of the unfolding method applied to mixtures of  $^{45}\text{Ca}$  and  $^{35}\text{S}$ . Activities for both radionuclides are large enough so that the background is negligible. Assays are distributed in groups of eight, each with similar activity ratios for  $^{45}\text{Ca}$  and  $^{35}\text{S}$ , which vary from 10/1 to 1/8. Each proportion is studied for SQP(E), which varies from 290 to 165. Table 2 shows that results for the same activity ratios are slightly better when  $^{45}\text{Ca}$  activity is greater than that of  $^{35}\text{S}$ . The calculation of  $^{45}\text{Ca}$  components is more difficult than the calculation of  $^{35}\text{S}$  components (compare samples 1–8 with samples 41–48 in Table 2), because  $^{45}\text{Ca}$  maximum  $\beta$  energy is greater than  $^{35}\text{S}$ ;  $^{45}\text{Ca}$  components appear narrower than  $^{35}\text{S}$  components for the same activity. Studies of different mixtures have shown that discrepancies for the less active nuclide depend on discrepancies for the more active nuclide. It was shown that nuclides with close maximum energies follow the expression

$$\delta_B = \frac{A_A}{A_B} \delta_A \quad (5)$$

where  $A_A$  and  $A_B$  are the activities for A and B radionuclides and  $\delta_A$  and  $\delta_B$  are their discrepancies, defined as

$$\delta_A = \frac{A_A^c - A_A}{A_A} \times 100 \quad (6)$$

where  $A_A^c$  is the computed activity and  $A_A$  the experimental activity. In  $^{45}\text{Ca}$  and  $^{35}\text{S}$  mixtures, the maximum  $\beta$  energy for the  $^{45}\text{Ca}$  nuclide is twice that of the  $^{35}\text{S}$  energy. Consequently, expression (5) is not applicable, and thus

$$\delta_B \leq \frac{A_A}{A_B} \delta_A \quad (7)$$

In general, we observed that for activity ratios <10, discrepancies for the less active nuclide are <10%. Figure 4 plots mixture 1 from Table 1 and its spectral components.

Table 3 shows results from mixtures of  $^{45}\text{Ca}$  and  $^{35}\text{S}$  with medium and low activities. The first group of six assays have close SQP(E), but the activity ratios change from one assay to another. They indicate that discrepancies <25% are obtained for the less active nuclide when activity ratios are >20. Results for medium activity are shown from rows 7 to 12. Samples were measured in half-hour periods. The results for low activities are shown from rows 13 to 16; samples were measured for 1 h. The spectral components from assay 14 are plotted in Figure 5. The spectra in

TABLE 2. Experimental and Computed Activities of <sup>45</sup>Ca and <sup>35</sup>S for Different Activity Ratios and Quench Parameters

Sample no.	Activity ratio <sup>45</sup> Ca/ <sup>35</sup> S	SQP(E)	Experimental activity (dpm)		Computed activity (dpm)		Discrepancy (%)	
			<sup>45</sup> Ca	<sup>35</sup> S	<sup>45</sup> Ca	<sup>35</sup> S	<sup>45</sup> Ca	<sup>35</sup> S
1	9.8/1	289.0	227988	23270	229021	23691	0.4	1.8
2	10.3/1	282.2	213898	20729	216718	19096	1.3	-7.9
3	9.8/1	267.9	227988	23270	228383	23275	0.2	0.02
4	10.3/1	254.2	213898	20729	213971	21577	0.03	4.1
5	10.0/1	243.4	221057	21998	222687	21493	0.7	-2.2
6	10.0/1	227.5	221057	21998	219218	22744	-0.8	3.4
7	10.3/1	198.7	214810	20894	213120	20664	-0.8	-1.1
8	10.3/1	171.3	214810	20894	215355	19594	0.3	-6.2
9	4.3/1	291.2	202656	46544	198187	49125	-2.2	5.5
10	4.7/1	283.6	180667	37693	180856	39819	0.1	5.6
11	4.3/1	268.5	202656	46544	202314	47712	-0.2	2.5
12	4.6/1	252.3	190131	41458	190084	40673	-0.02	-1.9
13	4.5/1	243.5	196495	43995	198101	41721	0.8	-5.2
14	4.5/1	227.7	196495	43995	196108	41747	-0.2	-5.1
15	4.6/1	199.1	190942	41788	189451	40561	-0.8	2.9
16	4.5/1	170.1	190942	41788	194661	36422	1.9	-12.8
17	1.6/1	290.1	151992	93089	153837	89257	1.2	-4.1
18	1.8/1	283.2	135500	75387	136764	75210	0.9	-0.2
19	1.6/1	267.3	151992	93089	152928	90444	0.6	-2.8
20	1.7/1	256.1	142598	82917	143555	80162	0.7	-3.3
21	1.6/1	243.2	147371	87990	148548	85330	0.8	-3.0
22	1.6/1	227.2	147371	87990	144408	88134	-2.0	0.2
23	1.7/1	198.1	143206	83576	143174	80663	-0.02	-3.5
24	1.7/1	171.2	143206	83576	143112	80270	-0.06	-3.9
25	1/1.4	289.5	101328	139633	101247	135997	-0.08	-2.6
26	1/1.3	284.2	90333	113080	90197	112361	0.1	-0.6
27	1/1.4	266.2	101328	139633	99077	138138	-2.2	-1.1
28	1/1.3	251.0	95065	124376	97006	120369	2.0	-3.3
29	1/1.3	243.3	98248	131986	103010	126413	4.8	-4.2
30	1/1.3	225.1	98248	131986	99203	127919	0.9	-3.1
31	1/1.3	196.9	95471	125364	93961	124853	-1.6	-0.4
32	1/1.3	168.9	95471	125364	98629	119492	3.3	-4.7
33	1/3.7	289.3	50664	186178	52947	179592	4.5	-3.5
34	1/3.5	283.0	47533	165834	47838	162297	0.6	-2.1
35	1/3.7	268.6	25332	209450	25019	201689	-1.2	-3.7
36	1/3.5	258.1	47533	165834	47250	163162	0.6	-1.6
37	1/3.6	243.3	49124	175981	48381	175281	-1.5	-0.3
38	1/3.6	228.8	49124	175981	47031	173330	-4.2	-1.5
39	1/3.5	198.7	47735	167152	46403	164697	-2.8	-1.5
40	1/3.5	169.9	47735	167152	48261	162432	1.1	-2.8
41	1/8.3	290.6	25332	209450	26801	200068	5.8	-4.4
42	1/7.5	283.8	22583	169621	23663	167184	4.8	-1.4
43	1/8.3	268.8	25332	209450	25019	201689	-1.2	-3.7
44	1/7.9	251.3	23766	186564	27453	179100	15.5	-7.1
45	1/8.1	243.1	24561	197979	25674	197127	4.5	-0.4
46	1/8.1	227.2	24561	197979	23270	195232	-5.2	-1.4
47	1/7.9	196.3	23867	188046	27161	181971	13.8	-3.2
48	1/7.9	169.7	23867	188046	21668	182495	-9.2	-2.9

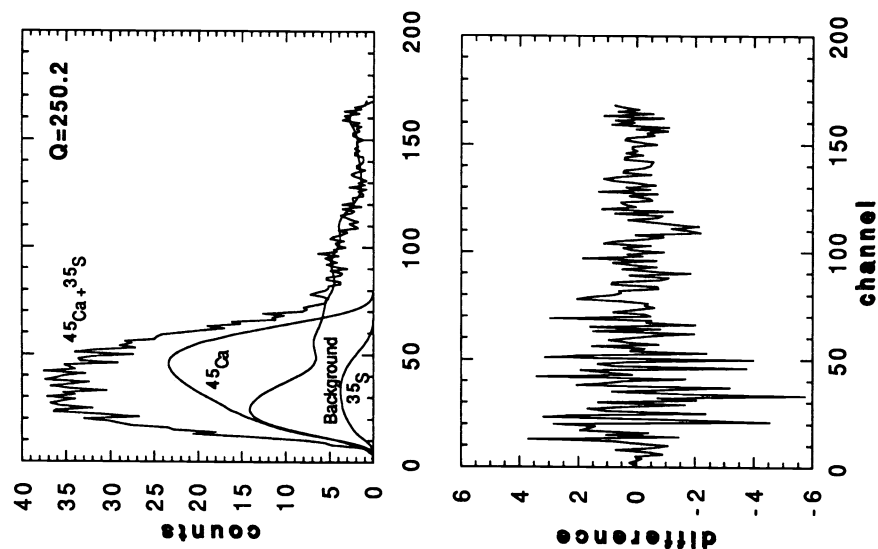


Fig. 5. Spectrum unfolding of sample 14 (Table 3) and difference spectrum

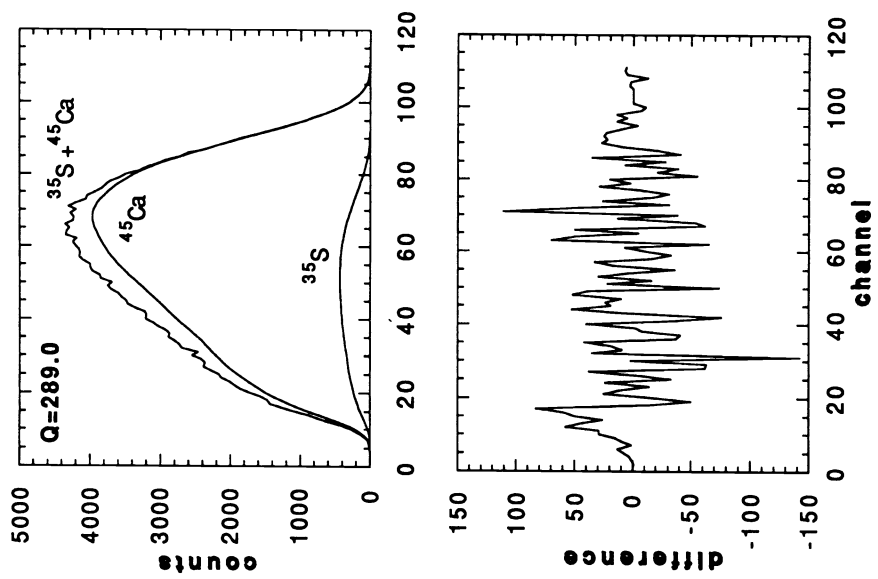


Fig. 4. Spectrum unfolding of sample 1 (Table 2) and difference spectrum

TABLE 3. Experimental and Computed Medium and Low Activities of  $^{45}\text{Ca}$  and  $^{35}\text{S}$  for Different Activity Ratios and Quench Parameters

Sample no.	Activity ratio	SQP(E)	Experimental activity (dpm)		Computed activity (dpm)		Discrepancy (%)	
			$^{45}\text{Ca}$	$^{35}\text{S}$	$^{45}\text{Ca}$	$^{35}\text{S}$	$^{45}\text{Ca}$	$^{35}\text{S}$
	$^{45}\text{Ca}/^{35}\text{S}$							
1	26.4/1	232.7	15443	586	15665	451	1.4	-23.0
2	1/20.9	227.4	638	13359	426	13965	-33.0	4.5
3	15.1/1	231.1	7721	512	8107	397	5.0	-22.0
4	1/12.0	230.8	558	6679	509	7081	-8.7	6.0
5	21.1/1	225.5	7721	366	8022	493	3.8	34.0
6	1/16.8	227.1	398	6679	217	7178	-45.0	7.4
7	1.6/1	255.0	466	297	469	298	0.6	0.3
8	4.2/1	255.0	622	149	642	123	3.2	-17.4
9	9.4/1	254.9	699	74	705	85	0.2	14.8
10	1/1.4	258.9	311	446	313	447	0.6	0.2
11	1/3.8	257.4	155	595	154	603	-0.6	1.3
12	1/8.7	253.4	77	669	75	680	-2.6	1.6
13	1.7/1	251.7	80	47	92	29	15.0	-38.0
14	4.6/1	250.2	106	23	108	16	2.0	-30.0
15	10/1	254.6	120	12	117	12	-2.0	1.0
16	1/1.3	250.9	53	70	64	55	20.0	-21.0
17	1/3.4	253.7	27	93	31	84	15.0	-9.0
18	1/8	258.1	13	104	17	92	30.0	-11.0

the plot were reduced 125% to show the background fitting at higher energies. The total background count rate was 80 cpm. From 13 to 15, the  $^{35}\text{S}$  counting rate is below the background, and from 16 to 18, is  $^{45}\text{Ca}$ . Discrepancies are *ca.* 30% for nuclides below background. These results agree with statistical fluctuations.

## CONCLUSIONS

We studied the influence of water on SQP(E) in scintillation gels and showed that calibration curves of counting efficiency *vs.* SQP(E) are the same for homogeneous and heterogeneous samples. We obtained experimental curves relating the quench parameter value to the amount of water or  $\text{CCl}_4$ . These curves allow one to prepare samples with a given SQP(E).

The CIEMAT/NIST method for homogeneous samples also can be applied to heterogeneous samples. This enables us to measure any nuclide independent of the chemical form and to use large amounts of aqueous solutions to avoid adsorption and precipitation. We also measured  $^{45}\text{Ca}$  and  $^{35}\text{S}$  mixtures for medium and low activities. As background has a spectral structure, it can be considered as another radionuclide; we can treat the mixture as a three-component system. We conclude that activities of nuclides with count rates below background can be determined with discrepancies within statistical uncertainties.

## ACKNOWLEDGMENTS

The authors would like to thank the reviewers for their suggestions and comments on the manuscript.

REFERENCES

- Coursey, B. M., Lucas, L. L., Grau Malonda, A. and García-Toraño, E. 1989 The standardization of Plutonium-241 and Nickel-63. *Nuclear Instruments and Methods in Physics Research A279*: 603–610.
- Grau Carles, A. and Grau Malonda, A. 1991a A new procedure for isotope analysis in liquid scintillation counting. In Ross, H., Noakes, J. E. and Spaulding, J. D., eds., *Liquid Scintillation Counting and Organic Scintillators*. Chelsea, Michigan, Lewis Publishers: 295–306.
- \_\_\_\_\_ 1991b Spectral interpolation and unfolding to measure multi-labelled samples in liquid scintillation. *CIEMAT Report 675*, Madrid, Spain
- Grau Carles, A., Martín-Casallo, M. T. and Grau Malonda, A. 1991 Spectrum unfolding and double-window methods applied to standardization of C-14 and H-3. *Nuclear Instruments and Methods in Physics Research A307*: 484–490.
- Grau Malonda, A. 1982a Metrología de la Radiactividad Beta Mediante el Recuento por Centelleo en Fase Líquida. Ph.D. Thesis 171/82. Department of Experimental Physics, Complutense University, Madrid: 175 p.
- \_\_\_\_\_ 1982b Counting efficiency for electron-capturing nuclides in liquid scintillator solutions. *International Journal of Applied Radiation Isotopes* 33: 371–375.
- Grau Malonda, A. and García-Toraño, E. 1982 Evaluation of counting efficiency in liquid scintillation counting of pure beta-ray emitters. *International Journal of Applied Radiation Isotopes* 33: 249–253.
- Günther, E. and Schötzig, U. 1992 Activity determination of Nb-93m. *Nuclear Instruments and Methods in Physics Research A312*: 132–135.
- Rodríguez, L., Los Arcos, J. M. and Grau, A. 1991 LSC standardization of <sup>32</sup>P in inorganic and organic samples by the efficiency tracing method. In Ross, H., Noakes, J. E. and Spaulding, J. D., eds., *Liquid Scintillation Counting and Organic Scintillators*. Chelsea, Michigan, Lewis Publishers: 593–609.